

# Comparison between Adjar and xDawn algorithms to estimate Eye-Fixation Related Potentials distorted by overlapping

Emmanuelle Kristensen<sup>1</sup>, Anne Guerin-Dugué<sup>1</sup> and Bertrand Rivet<sup>1</sup>

**Abstract**—Eye-Fixation Related Potentials technique is a joint analysis of both electrical brain activities and ocular movements. It permits to extract neural components synchronized with ocular fixations. But, the brain responses elicited by adjacent fixations can be distorted by overlapping process due to short inter fixations intervals. Two algorithms, Adjar and xDawn, are studied to correct these distortions. The Adjar performance is based on assumptions concerning the temporal distributions which become too restrictive for EFRP studies. On the contrary, the xDawn algorithm is based on a more general and flexible model which is well adapted to EFRP studies.

## I. INTRODUCTION

Event Related Potential (ERP) extraction is a very popular technique to study neural activities in response to specific events like stimulus presentation. Electroencephalographic (EEG) signals are time locked on specific events and then averaged. Thanks to ERP studies, a lot of neural potentials have been identified and associated to cognitive mechanisms. See [1] for a review at this date. But in order to avoid artifacts, during classical ERP experiments, participants must not move (muscular artifacts) and also have to fixate a given location on the screen to not move the eyes (ocular artifacts). For example, for reading studies, participants read word by word, a word at a time is displayed in the screen. This experimental context is far from natural reading ([2], [3]). The same observation is also for visual perception to study visual exploration of natural scenes ([4], [5], [6], [7]).

Recently, new techniques based on joint EEG and eye tracking (ET) acquisition, have been developed to allow a more ecological experimental framework. In one hand, the joint analysis of both electrical brain activities and ocular movements allows to study cognitive processes and their timeline, in ecological situations with more complex stimuli. The extracted Eye-Fixation Related Potentials (EFRP) are neural components synchronized with ocular fixations.

In other hand, EFRP technique has an important limitation to isolate time locked neural potentials. In fact, in most of the ERP experiments, inter stimuli intervals (ISI) can be managed to avoid overlapping between different time locked neural responses (the ISI are greater than the larger latency of the expected potentials). But in EFRP experiments, inter fixations intervals (IFI) depend on the temporal oculomotor

patterns of the participants. For example, the latency of the well-known P300 potential (around 300ms after the time locked trigger) is of the same order of magnitude as usual IFI (fixation plus saccade durations). Consequently, studying such potentials, in these natural experimental conditions, requires careful methodology to interpret the observed EFRPs.

To address this issue for ERP experiments, a first algorithm has been previously introduced: Adjacent Response Algorithm (“Adjar”) by Woldorff [8]. In the context of Brain Computer Interfaces, the “xDawn” algorithm [9] has been proposed for designing adapted spatial filters. We will show how this algorithm can be used as a new and flexible method to cope with overlapped EFRP waveforms.

In the following, both algorithms are introduced. Then, their performances are compared on different simulated realistic signals.

## II. ALGORITHMS FOR OVERLAPPING ISSUE

In this section, the overlapping issue is explained then both algorithms, Adjar and xDawn, are described.

### A. Overlapping issue

In the context of EFRP, most of the studies concern early potentials with latency less or about the average IFI (between 200 and 300ms depending on the task): P1 (latency between 80 and 100ms after the eye-fixations onset), N1 (latency between 130 and 250ms), P2 (latency between 200 and 300 ms), N2 (latency between 250 and 350ms) and P3 (latency between 300 and 500ms) [10]. In these conditions, with short latencies, overlapping distortions are neglected. For studies concerning late potentials: P3 (latency between 300 and 500ms), N400 (latency between 300 and 600ms), precautions are taken to avoid overlaps. For example, participants are trained to make longer fixations when exploring the visual scenes [7]. In these particular conditions, it might be objected that the experimental conditions are not natural.

Let  $x_i(t)$  denotes the response time-locked on the target fixation in the trial  $i$ :

$$x_i(t) = s_i(t) + s_{p,i}(t - \tau_{p,i}) + s_{s,i}(t - \tau_{s,i}) + n_i(t), \quad (1)$$

where  $s_i(t)$  denotes the response time-locked on target fixation for the trial  $i$ , at time index  $t$  and  $s_{p,i}(t)$  (resp.  $s_{s,i}(t)$ ) denotes the responses time-locked on immediately previous (resp. subsequent) fixation with  $\tau_{p,i}$  (resp.  $\tau_{s,i}$ ) the previous (resp. subsequent) fixation onset. Let  $n_i(t)$  denotes the ongoing brain activity which is not related to the fixations. The estimation  $\hat{s}(t)$  of the EFRP time-locked

\*This work was partially supported by a grant from the CNRS funding the PhD of Emmanuelle Kristensen.

<sup>1</sup> GIPSA-lab, Grenoble Images Parole Signal Automatique, UMR 5216 CNRS Grenoble Alpes, 11 rue des Mathématiques, Grenoble Campus, BP 46, F-38402 Saint Martin d’Hères Cedex (emmanuelle.kristensen; anne.guerin; bertrand.rivet)@gipsa-lab.grenoble-inp.fr

on target fixations is defined as the average on all trials ( $I$ ) for a given subject:

$$\hat{s}(t) = \frac{1}{I} \sum_{i=1}^I x_i(t). \quad (2)$$

Considering 1,  $\hat{s}(t)$  can then be rewritten as:

$$\hat{s}(t) = s(t) + D_p(t) * s_p(t) + D_s(t) * s_s(t) + n(t) \quad (3)$$

with  $*$  the convolutive product and  $s(t)$ ,  $s_p(t)$  and  $s_s(t)$  the average time-locked response elicited respectively on target fixations, on previous fixations and on the subsequent fixations.  $n(t)$  is the average of ongoing brain activity which is not related to fixations. Let  $D_p(t)$  and  $D_s(t)$  denote the normalized distributions of the IFIs ( $\tau_{p,i}$  and  $\tau_{s,i}$ ) with the previous and subsequent fixations, respectively.

So, if the IFIs are lower than latencies,  $\hat{s}(t)$  is additively noisy distorted by the previous overlapping response  $ov_p(t) = D_p(t) * s_p(t)$ , the subsequent overlapping response  $ov_s(t) = D_s(t) * s_s(t)$  and in all the cases, the remaining noise  $n(t)$ .

Two existing algorithms are applied to correct the EFRPs distortions: ‘‘Adjar’’ [8] and ‘‘xDawn’’ [9], [11].

### B. Adjar: general description

The Adjar algorithm iteratively estimates the average of previous and subsequent responses which are then subtracted to the target response, for the new iteration, and so on. The complete ‘‘Level 2 procedure’’, detailed in [8], is applied.

There are four main assumptions:

- 1) all stimuli elicit the same pattern  $s_p(t) = s_s(t) = s(t)$ ,
- 2) the model does not consider other ongoing brain activity  $n(t)$ , but only previous ( $ov_p(t)$ ) and subsequent responses ( $ov_s(t)$ ),
- 3) the principal causes of overlaps during the iterative process are due to the immediately adjacent responses (named first-order adjacent responses), and then,
- 4) the higher-order adjacent responses are considered as negligible, already from the second order ( $D_s(t) * D_s(t) * s(t)$ ,  $D_p(t) * D_p(t) * s(t)$ ).

At first sight, the first assumption seems to be the most restrictive one in the EFRP context, but it can be relaxed as done in the case of a Stop-Signal experiment [12]. For these experiments, ERPs elicited by the Stop event are distorted by responses elicited by the previous Go stimuli. Then, thanks to such straightforward adaptations, this procedure can be applied even when two different successive responses are overlapping. However, the overlap of three or more different responses, in a given observation interval, is not addressed by the Adjar algorithm. Here, the study will be focused on the two last assumptions.

The Adjar algorithm iteratively estimates the overlapping responses  $ov_p(t)$  and  $ov_s(t)$  from the evoked potential  $\hat{s}(t)$ . The  $k$ th iteration of the Adjar algorithm is described as:

$$\begin{aligned} \widehat{ov}_s^{(k)}(t) &= D_s(t) * (\hat{s}(t) - \widehat{ov}_p^{(k-1)}(t)), \\ \widehat{ov}_p^{(k)}(t) &= D_p(t) * (\hat{s}(t) - \widehat{ov}_s^{(k)}(t)), \end{aligned}$$

with  $\widehat{ov}_p^{(0)}(t) = 0$  and the estimation of  $s(t)$  after this iteration is given by :

$$\hat{s}^{(k)}(t) = \hat{s}(t) - \widehat{ov}_s^{(k)}(t) - \widehat{ov}_p^{(k)}(t). \quad (4)$$

At the last iteration, the remaining overlap in  $\hat{s}_{Adjar}(t) = \hat{s}^{(\infty)}(t)$  (4) contains two second order terms equal to  $D_s(t) * D_s(t) * s(t)$  and  $D_p(t) * D_p(t) * s(t)$ . These terms may not be necessarily neglected, depending on the temporal ranges of the distributions  $D_s(t)$  and  $D_p(t)$  as shown in Section IV.

### C. xDawn: general description

The objective of the xDawn method, described in [9], extended and theoretically analyzed in [11], was the design of adapted spatial filters to maximize the signal-to-noise ratio before classification.

Here for the overlapping issue, only the first part of this algorithm is adapted and used. For this, recorded signals (1) can be rewritten, using matrix notations to express the convolution, as:

$$\forall i \in \{1, \dots, I\}, \quad \mathbf{x}_i = Q_i \mathbf{s}_i + Q_{p,i} \mathbf{s}_{p,i} + Q_{s,i} \mathbf{s}_{s,i}, \quad (5)$$

where  $\mathbf{x}_i = [x_i(1), \dots, x_i(T_i)]^\dagger \in \mathbb{R}^{T_i}$ , with  $T_i$  the number of time samples of the  $i$ th trial and  $\dagger$  the transpose operator.  $\mathbf{s}_i \in \mathbb{R}^{T_i}$ ,  $\mathbf{s}_{p,i} \in \mathbb{R}^{T_p}$  and  $\mathbf{s}_{s,i} \in \mathbb{R}^{T_s}$  are the vectors of the response time-locked on the target fixation, on the previous fixation and on the subsequent fixation, respectively.  $T_t$ ,  $T_p$  and  $T_s$  are the lengths of the responses  $s_i(t)$ ,  $s_{p,i}(t)$  and  $s_{s,i}(t)$ , respectively. Finally,  $Q_i$ ,  $Q_{p,i}$  and  $Q_{s,i}$  are Toeplitz matrices defined by their first column whose all entries are zero but the entries related to  $t = 0$ ,  $t = \tau_{p,i}$  and  $t = \tau_{s,i}$  equal to one, respectively. Consequently, all the trials can be concatenated to obtain:

$$\mathbf{x} = Q\mathbf{s} + Q_p \mathbf{s}_p + Q_s \mathbf{s}_s, \quad (6)$$

with  $\mathbf{x} = [\mathbf{x}_1^\dagger, \dots, \mathbf{x}_I^\dagger]^\dagger$  and  $Q = [Q_1^\dagger, \dots, Q_I^\dagger]^\dagger$ ,  $Q_p = [Q_{p,1}^\dagger, \dots, Q_{p,I}^\dagger]^\dagger$  and  $Q_s = [Q_{s,1}^\dagger, \dots, Q_{s,I}^\dagger]^\dagger$ . By least square minimization, one can estimate in a close form the average responses time-locked on respectively the target, the previous, and the subsequent fixations ( $\hat{\mathbf{s}}$ ,  $\hat{\mathbf{s}}_p$ ,  $\hat{\mathbf{s}}_s$ ) by:

$$[\hat{\mathbf{s}}^\dagger, \hat{\mathbf{s}}_p^\dagger, \hat{\mathbf{s}}_s^\dagger]^\dagger = (B^\dagger B)^{-1} B^\dagger \mathbf{x}, \quad (7)$$

with  $B = [Q, Q_p, Q_s]$ .

## III. METHODOLOGY

This section presents the methodology to simulate the database used for the application and the comparison of the two algorithms.

### A. General principles

The final aim of this study is to apply both algorithms in realistic EFRP contexts. The simplest case of overlapping is considered, as described in (1), and under the first assumption ( $s_p(t) = s_s(t) = s(t)$ ). In a first step, the  $D_s$  and  $D_p$  distributions are completely controlled in order to have a base line for the comparison. In a second step, the  $D_s$  and  $D_p$  distributions are extracted from a real experiment to be in realistic conditions for EFRPs extraction. Moreover, to obtain

a “ground truth” for comparison, the algorithms are applied on the same simulated waveforms, generated to be similar to EEG signals.

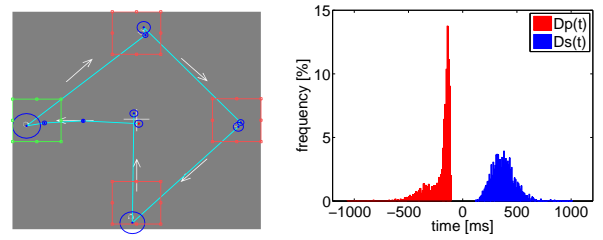
### B. Parameters for simulated data

1) *Different distributions*: In order to evaluate the impact of the temporal range of the  $D_p$  and  $D_s$  distributions on the algorithms’ effectiveness, two groups of simulation were realized.

For the first group, the  $D_p$  and  $D_s$  distributions were uniform distributions between -950ms and -800ms and between 800ms and 950ms, respectively. The time,  $t=0$ ms, is the time locked on the target fixation, the fixation of interest in each trial. Let “Case 1” denote this group of distributions.

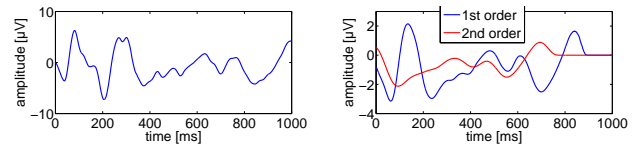
For the second group, the  $D_p$  and  $D_s$  distributions were directly extracted from an experiment of visual search. EEG and eye-tracking signals were jointly recorded for ten healthy participants. The goal of the experiment was to detect if there was or not one or more target stimuli among the four stimuli displayed on the screen. The participants were asked to follow a given pattern during 2.7 sec for each trial. The scanpath (figure 1(a)) shows the path of an eye during a trial. In this figure, the stimuli are overlapped by circles which represent eye-fixations. The green and red rectangles around the stimuli define the regions of interest (ROI). In this example, there was one target stimulus (inside the green ROI) and three no-target stimuli inside the red ROI. For the analysis, all fixations with a duration shorter than 90ms were suppressed. If more than one fixation were landed on a target stimulus, the fixation with longest duration was chosen, the mean duration was 350ms. After pre-processing (trial segmentation, artifacts and noisy trials rejection), the mean number of trials was 242 by subject. The  $D_p$  and  $D_s$  distributions were then extracted from eye-tracking data (figure 1(b)). The time was locked on the target fixation’s onset. The mean latency of immediately previous (resp. subsequent) fixation was -207ms (resp. 376ms). The  $D_p$  distribution was mainly explained by the duration of the previous fixations whose a major proportion was landed between two ROIs and was very short (in average 151ms). To obtain the IFI distribution, the duration of the output saccade was added (stable delay). For the  $D_s$  distribution, the duration of the target fixations was longer. That explains the different aspects of  $D_p$  and  $D_s$  distributions. Let “Case 2” denote this group of distributions.

The validity of the fourth assumption for Adjar (i.e: the second-order adjacent responses are negligible) depends on the temporal range of distributions. For Case 1,  $D_p(t) * D_p(t) * s(t)$  was between -1800ms and -1700ms and  $D_s(t) * D_s(t) * s(t)$  between 1700ms and 1900ms. So, in this case, the second-order responses were really outside the observation windows defined on  $[0; 1000]ms$ . In Case 2,  $D_p(t) * D_p(t) * s(t)$  (resp.  $D_s(t) * D_s(t) * s(t)$ ) was between -2134ms and -212ms (resp. between 232ms and 2026ms). A part of the second-order responses were included in the observation windows. Thanks to these two cases, we were

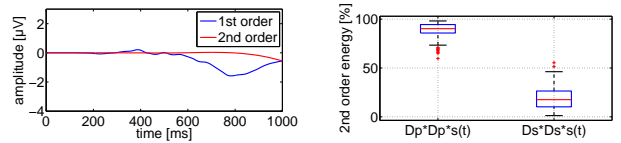


(a) Eye scanpath during a trial. (b)  $D_p$  and  $D_s$  distributions from the target fixation onset

Fig. 1. Scanpath and distributions from real joint EEG and ET acquisitions. In (a), the circles represent the fixation positions, the radius and their duration. The boxes are the ROIs including the target or the non target stimulus.



(a) Example of an original waveform  $s(t)$  (b) First and second order previous responses



(c) First and second order subsequent responses (d) Part (%) of the energy of second order responses in the observation windows

Fig. 2. For Case 2 : Example of signals (original waveform, first and second order responses), and importance (%) of second order response.

able to analyse the impact of the second-order adjacent responses on the signal assesment.

2) *Generation of simulated signals*: The modelisation for the observed signal is given by (3), with  $s_p(t) = s_s(t) = s(t)$  to be in the best configuration for Adjar algorithm. A waveform,  $s(t)$  was randomly generated (figure 2(a) for one trial). White noise was added to the generated waveform to simulate other ongoing brain activity as described in (1). The mean SNR was -0.35dB. The observation windows was between 0ms and 1000ms and the sampling frequency was 1000 Hz. Each configuration was repeated 1000 times, for a statistical evaluation of the mean squared error on the final estimation.

Figures 2(b) and 2(c) illustrate for Case 2, the second order responses, but also the first order ones. And more precisely, 88% on average of the second-order previous responses energy and 19% on average of the second-order subsequent responses energy were in the observation windows (figure 2(d)). For reasons of space, similar graphs for Case 1 are not presented here, the energy of second order previous (resp. subsequent) response was null inside the observation window. These results were in accordance with our remarks on the second order distributions. In other terms, for Case 1, all the Adjar’s asumptions were verified, and for Case 2

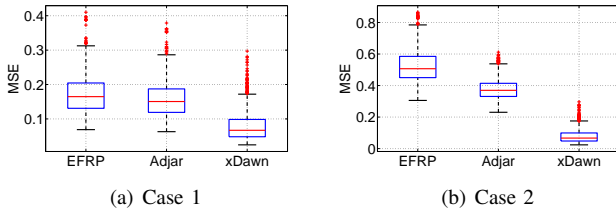


Fig. 3. Boxplot of the mean squared error for the three algorithms extracting EFRP, in both cases.

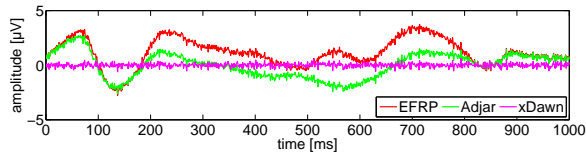


Fig. 4. For Case 2 : Comparison of EFRP estimation; for each method, temporal evolution of the instantaneous estimation error  $s(t) - \hat{s}(t)$  from the original signal illustrated at figure 2(a).

the Adjar’s fourth assumption was not verified. Nevertheless, this last case is more encountered in the EFRPs studies.

#### IV. RESULTS AND DISCUSSION

The simple averaging, Adjar and xDawn estimations were compared with the two types of  $D_p$  and  $D_s$  distributions. The main difference between Case 1 and Case 2 concerns their temporal range. Overall, the MSE is better for Case 1 than for Case 2 (figure 3). In fact for Case 1, the EFRP at the target fixation onset is less distorted while previous fixations occur earlier and subsequent fixations occur later than for Case 2 (realistic distributions). In this Case 1, the three techniques have succeeded to correctly estimate the signal, their performance is correct and similar. For Case 2, where IFI are lower, the situation is different. There are more overlaps. We observed an increasing MSE from Case 1 to Case 2 more particularly when extracting neural potentials by simple averaging or by applying Adjar (See figure 4 for the instantaneous error). This performance degradation is due to the overlapping amount as it is expressed by a significant part of the second order energy in the observation window (figure 2(d)). In both cases, the xDawn performance is better, and the performance enhancement compared to the two others algorithms is significant for Case 2. Moreover the xDawn performance remains stable and is not impacted by the overlapping amount. This is in accordance with the general model described by (6). These results show that xDawn is not sensitive to the different types of distribution, unlike Adjar.

#### V. CONCLUSION AND PERSPECTIVES

In this paper, two algorithms are compared, Adjar and xDawn, to correct distortions of Eye-Fixation Related Potential due to overlap of adjacent fixations responses. The algorithms were applied on simulated data but with realistic distributions of fixations latencies. Our simulations show that xDawn is more efficient and robust to correct distortions of

Eye-Fixation Related Potential. The Adjar performance is based on assumptions concerning the temporal IFI distributions which become too restrictive for EFRP studies. On the contrary, the xDawn algorithm is based on a more general and flexible model which is well adapted to EFRP studies. There is no assumption on the temporal IFI distributions and on the similarity or not of the neural responses elicited by the different fixations in the observation window. Works are ongoing with the real EEG signals on this visual search experiment to confirm these results. And very promising results have been already obtained with real EEG signals obtained during an exploration visual task [13].

#### ACKNOWLEDGMENT

The softwares for the experiment and eye tracking data processing were developed by Gelu Ionesco and Anton Andreev. The authors would like to thank the “Délégation à la Recherche Clinique et à l’Innovation” of the CHU “Centre Hospitalier Universitaire” of Grenoble for their role in the ethics committee.

#### REFERENCES

- [1] A. P. F. Key, G. O. Dove, and M. J. Maguire, “Linking brainwaves to the brain: an erp primer,” *Developmental neuropsychology*, vol. 27, no. 2, pp. 183–215, 2005.
- [2] A. Frey, G. Ionescu, B. Lemaire, F. López-Orozco, T. Baccino, and A. Guérin-Dugué, “Decision-making in information seeking on texts: an eye-fixation-related potentials investigation,” *Frontiers in systems neuroscience*, vol. 7, 2013.
- [3] O. Dimigen, W. Sommer, A. Hohlfield, A. M. Jacobs, and R. Kliegl, “Coregistration of eye movements and eeg in natural reading: analyses and review,” *Journal of Experimental Psychology: General*, vol. 140, no. 4, p. 552, 2011.
- [4] A.-M. Brouwer, B. Reuderink, J. Vincent, M. A. van Gerven, and J. B. van Erp, “Distinguishing between target and nontarget fixations in a visual search task using fixation-related potentials,” *Journal of vision*, vol. 13, no. 3, p. 17, 2013.
- [5] A. Lou and P. Sajda, “Do we see before we look?” in *Neural Engineering, 2009. NER’09. 4th Int. IEEE/EMBS Conf. on*. IEEE, 2009, pp. 230–233.
- [6] G. Healy and A. F. Smeaton, “Eye fixation related potentials in a target search task,” in *Engineering in Medicine and Biology Society, EMBC, 2011 Annual Int. Conf. of the IEEE*. IEEE, 2011, pp. 4203–4206.
- [7] L. N. Kaunitz, J. E. Kamienkowski, A. Varatharajah, M. Sigman, R. Q. Quiroga, and M. J. Ison, “Looking for a face in the crowd: Fixation-related potentials in an eye-movement visual search task,” *NeuroImage*, vol. 89, pp. 297–305, 2014.
- [8] M. G. Woldorff, “Distortion of erp averages due to overlap from temporally adjacent erps: analysis and correction,” *Psychophysiology*, vol. 30, no. 1, pp. 98–119, 1993.
- [9] B. Rivet, A. Souloumiac, V. Attina, and G. Gibert, “xDawn algorithm to enhance evoked potentials: application to brain–computer interface,” *Biomedical Engineering, IEEE Transactions on*, vol. 56, no. 8, pp. 2035–2043, 2009.
- [10] S. J. Luck, *An introduction to the event-related potential technique*. MIT press, 2014.
- [11] B. Rivet and A. Souloumiac, “Optimal linear spatial filters for event-related potentials based on a spatio-temporal model: Asymptotical performance analysis,” *Signal Processing*, no. 2, pp. 387 – 398, February.
- [12] E. M. Bekker, J. L. Kenemans, M. R. Hoeksma, D. Talsma, and M. N. Verbaten, “The pure electrophysiology of stopping,” *International Journal of Psychophysiology*, vol. 55, no. 2, pp. 191–198, 2005.
- [13] H. Devillez, E. Kristensen, N. Guyader, B. Rivet, and A. Guérin-Dugué, “The P300 potential for fixations onto target object when exploring natural scenes during a visual task after denoising overlapped EFRP,” 2015, submitted to the 7th Int. IEEE/EMBS Conf on. Neural Engineering.